HOKKAIDO UNIVERSITY

Title	Meniscus extrusion and lower leg alignment predict the distribution of subchondral bone density across the knee joint
Author(s)	Iwasaki, Koji; Ebata, Taku; Sato, Tomoya et al.
Citation	Knee, 57, 68-76 https://doi.org/10.1016/j.knee.2025.07.020
Issue Date	2025-08-19
Doc URL	https://hdl.handle.net/2115/98335
Rights	© 2025. This manuscript version is made available under the CC-BY-NC-ND 4.0 license https://creativecommons.org/licenses/by-nc-nd/4.0/
Rights(URL)	https://creativecommons.org/licenses/by-nc-nd/4.0/
Type	journal article
File Information	manuscript.pdf

Hokkaido University Collection of Scholarly and Academic Papers

Hokkaido University Collection of Scholarly and Academic Papers : HUSCAP

Meniscus extrusion and lower leg alignment predict the distribution of subchondral bone density across the knee joint

Koji Iwasaki[1*], Taku Ebata[2], Tomoya Sato[2], Yoshiaki Hosokawa[2], Masanari Hamasaki[2], Dai Sato[2], Masatake Matsuoka[2], Tomohiro Onodera[2], Eiji Kondo[3], Norimasa Iwasaki[2]

[1] Department of Functional Reconstruction for the Knee Joint, Faculty of Medicine, Hokkaido University, North-15, West-7, Sapporo, Hokkaido 060-8638, Japan

[2] Department of Orthopedic Surgery, Faculty of Medicine and Graduate School of Medicine, Hokkaido University, North-15, West-7, Sapporo, Japan

[3] Centre for Sports Medicine, Hokkaido University Hospital, North-15, West-6, Sapporo, Japan

*Corresponding Author: Koji Iwasaki, MD, PhD

Department of Functional Reconstruction for the Knee Joint, Faculty of Medicine, Hokkaido University, North-15, West-7, Sapporo, Hokkaido 060-8638, Japan

Telephone: +81-11-706-5935, Fax: +81-11-706-6054.

E-mail: koji.iwasaki@elms.hokudai.ac.jp

Running title: Alignment and Meniscus Predict Stress

Keywords: Osteoarthritis, Meniscus extrusion, Lower limb alignment, Subchondral bone density

Abstract

Background: Stress distribution is the pattern of mechanical load distribution, particularly between the medial and lateral compartments. Lower leg alignment and the meniscus play an important role in this distribution. CT-osteoabsorptiometry estimates stress distribution by analyzing the distribution pattern of subchondral bone density. This study aimed to explore the extent to which lower limb alignment and meniscal extrusion can explain the distribution of subchondral bone density.

Methods: This was a retrospective study including 92 patients (73 with osteoarthritis (OA) and 19 without OA). Lower limb alignment, meniscus-extrusion ratio (MER), and subchondral bone density were assessed using CT-osteoabsorptiometry. High-density areas (HDA) on the articular surface were quantitatively analyzed.

Results: Hip-knee-ankle (HKA) angle, medial MER (MMER), lateral MER (LMER), and medial compartment HDA to total HDA ratio (medial ratio) were −4.3°, 46.8%, 20.4%, and 70.0%, respectively. Multiple regression analysis revealed that HKA, MMER, and LMER were significant variables. The adjusted R2 of HKA, MMER, and LMER for the medial ratio was 0.80. The standardized coefficients for HKA, MMER, and LMER were −0.30, 0.40, and −0.41, respectively.

Conclusions: Lower leg alignment and meniscus extrusion explain 80% of the variance in the distribution of subchondral bone density. These findings indicate that both factors can account for approximately 80% of the estimated stress distribution as assessed by CT-osteoabsorptiometry. The distribution of subchondral bone density estimated by HKA and meniscus extrusion was useful for diagnosing and treating knee osteoarthritis.

Introduction

Knee osteoarthritis (OA) is associated with aging, gender, genetics, obesity, malalignment, and trauma [1, 2]. Among them, malalignment and breakdown of the hoop function following meniscal injury have been reported to cause localized overstress on the knee joint surface, leading to cartilage wear [1, 2]. Therefore, identifying the stress distribution on the knee joint surface in each patient is crucial to identifying areas of overstress, leading to early treatment interventions, such as high tibial osteotomy (HTO), and preventing OA progression.

However, directly clarifying the stress distribution across the knee joint in individual patients is challenging. Therefore, stress distribution has been estimated using various methods, such as three-dimensional (3D) motion analysis, biomechanical studies using cadavers, and finite element analysis. Furthermore, studies have been conducted using load sensor-integrated implants in total knee arthroplasty (TKA). This method was thought to be the only approach that allowed the direct measurement of the stress distribution. However, this method did not allow direct measurement of individual stress distribution, and meniscus function was not considered.

Based on Wolff's law, which claims that bone strength is enhanced in areas under high stress, resulting in increased mineralization [3], bone density is a substitute for direct stress measurements. Bone mineral density of the mediolateral compartment has been reported to correlate with knee adduction moment (KAM) [4, 5], which is a surrogate of mediolateral loading in the knee joint[6], indicating that the mediolateral distribution of bone density may adapt in response to stress on the articular surface. CT-osteoabsorptiometry (CT-OAM) is an analytical method for estimating the stress distribution on the living joint surface based on the distribution of

subchondral bone density across the articular cartilage [7]. Previous studies have demonstrated a correlation between the mediolateral distribution of subchondral bone density and leg alignment [8]. Furthermore, changes in leg alignment due to HTO result in changes in the distribution of subchondral bone density [8, 9]. However, the mechanism by which the distribution of subchondral bone density reflects the stress distribution has not been fully elucidated.

Lower leg alignment and meniscus hoop function are important factors affecting stress distribution [1, 2]. Furthermore, leg alignment strongly interacts with meniscus dysfunction [10], indicating that even with the same leg alignment, the stress distribution may differ if the meniscus status is different. Therefore, a method in which both leg alignment and the meniscus are evaluated simultaneously may enable the estimation of the stress distribution. Meniscus extrusion, which is the displacement of the meniscus medially or laterally outside the margins of the tibial plateau, has recently been recognized as a hallmark of meniscus dysfunction [11]. It can result from various types of meniscal tears, particularly radial and root tears. Reported risk factors include increasing age, malalignment, degenerative joint changes, high body mass index, and female sex [12]. This study aimed to clarify the extent to which the distribution of subchondral bone density measured by CT-osteoabsorptiometry can be explained by lower leg alignment and meniscus extrusion. Furthermore, this study aimed to investigate the validity of the relationship between the distribution of subchondral bone density and stress distribution by making a comparison with previous reports. We hypothesized that leg alignment and meniscus extrusion could explain the distribution of subchondral bone density across the knee joint.

77 **Method**

78 This study was approved by the Institutional Review Board of Hokkaido university Hospital (No.: #018-0213),
79 and it included patients who underwent osteotomy around the knee for OA and knee trauma between 2016 and
80 2021 at Hokkaido university hospital. Radiographic, CT, and MRI examinations were retrospectively analyzed.
81 Patients with a wide range of lower limb alignments, including both varus and valgus deformities, were included
82 to evaluate how alignment patterns, in conjunction with meniscal extrusion, influence the distribution of
83 subchondral bone density. Data on the ipsilateral side of the knees in patients with OA were obtained. This
84 population was selected because, at our institution, patients undergoing osteotomy represent the largest group
85 for whom both CT and MRI of the knee are routinely available. Importantly, only preoperative imaging data
86 were used for analysis to evaluate the relationship between meniscus extrusion, lower limb alignment, and
87 subchondral bone density. Moreover, data on the contralateral knees of patients with knee trauma were used as
88 non-OA controls. In addition, data from the contralateral knees of patients with unilateral knee
89 trauma were used as non-OA controls. At our institution, CT and MRI imaging of the contralateral
90 (uninjured) knee is routinely requested for patients with knee trauma as a surveillance measure.
91 Furthermore, based on the exclusion criteria described below, we ensured that these contralateral
92 knees showed no clinical or radiographic signs of OA, thereby allowing us to assess the distribution
93 of subchondral bone density in healthy joints. Exclusion criteria were as follows: (1) osteotomy around
94 the knee performed for other diagnoses such as spontaneous osteonecrosis of the knee joint, (2) previous surgery
95 at the evaluated knee, (3) lack of radiographic, CT, and MRI examinations, and (4) nonradiographic OA at the

96 contralateral side of the knees in patients with knee trauma. Of the 102 patients who underwent osteotomy around
97 the knee for OA during the study period, 29 were excluded. Of the 94 patients who underwent contralateral knee
98 trauma surgery, 75 were excluded. Finally, 92 knees of 92 patients (59 with varus OA, 14 with valgus OA, and
99 19 with contralateral knee trauma [non-OA]) were included in this study.

100 Full-length anteroposterior radiographs of the lower limb in full extension were obtained for
101 radiographic evaluation. Radiological parameters were evaluated preoperatively, including the degree of OA at
102 the tibiofemoral joints assessed using the Kellgren–Lawrence classification of the weight-bearing
103 anteroposterior radiographs of the femorotibial joint [13], and hip–knee–ankle angle (HKA; varus was negative),
104 percentage of mechanical axis, mechanical lateral distal femoral angle (mLDFA), and mechanical medial
105 proximal tibial angle (mMPTA) measured on anteroposterior radiographs of the whole lower limb taken with a
106 long cassette in the one-leg standing position.

107

108 *Meniscus status evaluation*

109 Meniscus extrusion was evaluated using coronal T2-weighted images acquired at 3.0-mm intervals
110 using a 3.0 Tesla MRI scanner (Discovery MR750W 3.0T, GE Healthcare. Chicago, USA). The location of the
111 medial meniscus (MM) on the joint line was quantified based on a previous study [14]. Briefly, a vertical line
112 intersecting the peripheral margin of the medial tibial plateau was drawn on the coronal image at the midpoint
113 of the superficial layer of the medial collateral ligament (Fig. 1). Two additional lines were drawn parallel to the
114 first line at the outer (periarticular) and inner (intra-articular) margins of the meniscus, respectively. The distance

between the first and second lines, defined as “extrusion width (EW),” and the distance between the second and third lines, defined as “total width (TW),” were measured. The medial meniscus-extrusion ratio (MMER) was calculated as EW / TW. The same method was applied to the lateral meniscus, which was evaluated as the lateral meniscus-extrusion ratio (LMER). The locations of MM and LM on the joint line in each group were independently measured by two orthopedic surgeons (TE and TS).

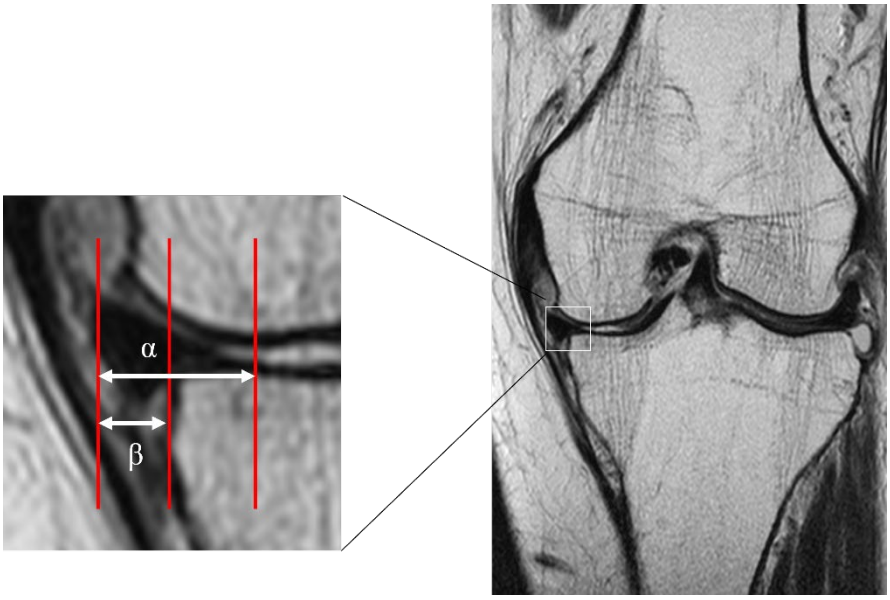

Fig. 1. Measurement of the location of the medial meniscus (MM) on the coronal image of the left knee on magnetic resonance imaging. A vertical line (solid line) intersecting the peripheral margin of the medial tibial plateau was drawn. The second (dotted line) and third lines (dashed line), parallel to the first line, were drawn at the outer and inner margins of the meniscus, respectively. Distance between the first and second lines, defined as the “extrusion width (EW),” and the distance between the second and third lines, defined as the “total width (TW),” were measured; each width was quantified in millimeters.

CT-osteoabsorptiometry

Axial images of the knee were acquired with a slice thickness of 0.5 mm using a high-resolution helical CT scanner (Aquilion One/ViSION Edition; Toshiba Medical Systems, Japan). Acquired CT data were transferred to a personal computer. Sagittal and coronal slices at 1.0-mm intervals and 3D bone models were

generated from axial CT data using commercial software (Ziocube®; Ziosoft, Inc., Tokyo, Japan). The sagittal and coronal axes were determined based on the epicondylar axis of the distal femoral condyle at the axial slice. An outline of the medial and lateral compartment of the proximal tibial articular surface was manually selected to include the entire subchondral bone layer of the articular surface in all slices based on sagittal and coronal CT images and a 3D CT image of the articular surface of the proximal tibia [8, 15]. The subchondral bone density of each generated sagittal slice was then analyzed using noncommercial software (Osteodens 4.0) [15-18]. The maximum increment point in Hounsfield units from the joint surface was selected as the starting point of the region of interest, and the maximum point in Hounsfield units was selected automatically in the 2.5-mm region of interest from the starting point. The radiodensity of the identified subchondral bone region was determined at each coordinate point at 1-mm intervals. Sagittal slices were then stacked, and a two-dimensional image that mapped the distribution of subchondral bone density was created (Fig. 2). The range between the maximum and minimum values in Hounsfield units on the mapping images was divided into nine grades, which were used to generate a surface mapping image and produce a color scale in which red and violet indicated the greatest and lowest bone densities, respectively.

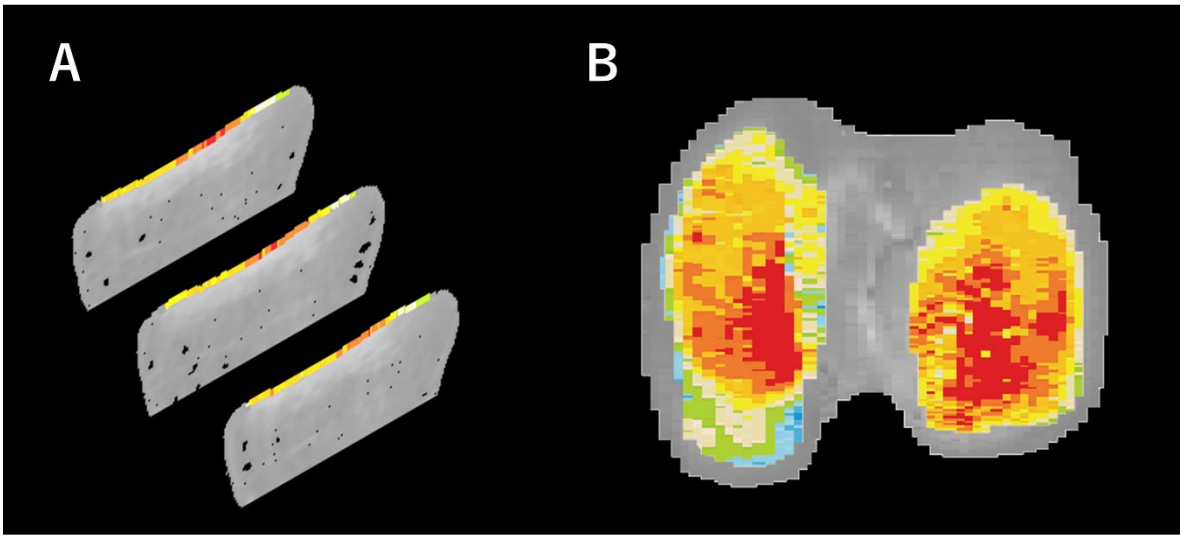

Fig. 2. Measurement of subchondral bone density in the proximal tibia using customized software. (A) The subchondral bone density of the selected area was automatically measured at each coordinate point in each 1.0-mm sagittal slice. (B) Map of the subchondral bone density distribution created by stacking sagittal slice data.

The obtained mapping data were quantitatively analyzed, focusing on the location of the high-density area (HDA) of the articular surface, which was defined as the region containing the coordinate points representing the top 20% of the Hounsfield unit values out of the total area of the medial and lateral compartments. The ratio of the HDA of the medial compartment to the total HDA of both compartments was calculated as the medial ratio [8].

%HDA was assessed by two observers (TE and TS). Intra- and interobserver reliability were evaluated on five randomly selected knees. The intraobserver reproducibility of the medial ratio measured using CT-OSTEOABSORPTIOMETRY showed interclass correlation coefficients (ICC) for intraobserver agreement of 0.916 for TE and 0.910 for TS. The ICC for interobserver reproducibility of the medial ratio was 0.904.

Statistical analysis

Statistical analyses were performed using JMP Pro 17.0 (SAS Institute Inc., Cary, 256 NC, USA). The

relationship between the medial ratio and various explanatory variables, including the MER and lower limb alignment, was analyzed using simple linear regression and multiple regression analyses. Simple linear regression analyses were performed for each explanatory variable to explore their separate effects on the medial ratio. Subsequently, a multiple regression analysis was performed to evaluate the combined effects of all explanatory variables on the medial ratio. Multicollinearity among the explanatory variables was assessed using the variance inflation factor (VIF). Variables with VIF values >5 were excluded from the final multiple regression model to ensure reliable coefficient estimates. A p-value = 0.05 indicated statistical significance. The post hoc power analysis revealed that, with an alpha value of 0.05 and a sample size of 92 knees, a power of 0.98 was achieved for the multiple regression analysis of the medial ratio.

Results

A total of 92 patients were included in this study. Of the 92 patients, varus OA patients were 59, valgus OA patients were 14, and non-OA were 19. The mean HKA for all patients was −4.3° (95% CI: −5.5 to −3.1). Subgroup analysis showed that the mean HKA was −7.4° (−8.4 to −6.4) in varus OA patients, 6.0° (4.4 to 6.4) in valgus OA patients, and −2.1° (−3.2 to −1.0) in non-OA patients. The mean MMER and LMER for all patients were 46.7% (95% CI: 40.1 to 52.7) and 20.3% (15.5 to 25.2), respectively. In subgroup analysis, MMER was 64.8% (60.1 to 69.6) in varus OA, 17.1% (10.9 to 23.2) in valgus OA, and 12.5% (9.2 to 15.7) in non-OA patients. The corresponding LMER values were 13.7% (11.7 to 15.7), 65.2% (46.7 to 83.7), and 5.7% (5.2 to 10.3), respectively. The mean LMER for all patients was 20.3% (95% CI: 15.5 to 25.2). Subgroup analysis showed

that LMER was 13.7% (11.7 to 15.7) in varus OA, 65.2% (46.7 to 83.7) in valgus OA, and 5.7% (5.2 to 10.3) in non-OA patients. The mean medial ratio was 70.0% (95% CI: 65.5 to 74.5) for all patients, 75.0% (71.1 to 78.8) in varus OA, 48.9% (42.5 to 55.2) in valgus OA, and 38.3% (33.7 to 42.9) in non-OA patients (Table 1).

Table 1. Patient characteristics.

	All patients (n=92)		Varus OA patients (n=59)		Valgus OA patients(n=14)		Non-OA patients (n=19)	
	Mean	95% CI	Mean	95% CI	Mean	95% CI	Mean	95% CI
Age (years)	51.1	[48.3, 53.9]	56.9	[54.6, 59.2]	47.4	[38.3, 56.5]	35.7	[30.1, 41.4]
Sex (n Male : n Female)	40 : 52		27 : 32		5 : 9		8: 11	
Height (cm)	162.4	[160.4, 164.5]	160.6	[158.0, 163.1]	168.3	[159.2, 177.3]	165.7	[162.1, 169.3]
Weight (kg)	72.1	[68.8, 75.4]	73.6	[69.6, 77.5]	68.1	[50.4, 85.9]	69.3	[63.0, 75.5]
HKA (°)	−4.3	[−3.1, −5.5]	−7.4	[−8.4, −6.4]	6.0	[4.4, 6.4]	−2.1	[−3.2,−1.0]
mLDFA (°)	86.7	[86.3, 87.2]	87.5	[87.1, 87.8]	83.5	[82.5, 84.4]	86.7	[86.2, 87.6]
mMPTA (°)	84.3	[83.6, 84.9]	82.8	[82.1, 83.5]	88.1	[87.3, 89.0]	85.9	[84.8, 87.0]
Ratio of meniscus extrusion (%)								
Medial meniscus	46.7	[40.1, 52.7]	64.8	[60.1, 69.6]	17.1	[10.9, 23.2]	12.5	[9.2, 15.7]
Lateral meniscus	20.3	[15.5, 25.2]	13.7	[11.7, 15.7]	65.2	[46.7, 83.7]	8.0	[5.7, 10.3]
Medial ratio (%)	70.0	[65.5, 74.5]	81.8	[79.5, 84.2]	31.2	[18.5, 43.9]	62.0	[57.7, 66.3]

Data are presented as means (95% CI). Non-OA, contralateral knee of the trauma; HKA, hip–knee–ankle angle; mLDFA, mechanical lateral distal femoral angle; mMPTA, mechanical medial proximal tibial angle; EW, extrusion width of the meniscus; TW, total width of the meniscus.

The single linear regression analysis at all subjects revealed significant correlations between the medial ratio and HKA ($R^2 = 0.63$), mLDFA (0.36), mMPTA (0.38), MMER (0.45), and LMER (0.47) ($p < 0.001$) (Table 2). The mMPTA had a VIF of ≥5 and was excluded from the multiple regression analysis. The multiple regression analysis of all subjects revealed that HKA, MMER, and LMER were significant independent variables with regression coefficient (β) of −0.01, 0.30, and −0.38, respectively ($p < 0.01$) (Table 3). The standardized regression coefficients of MMER (0.40) and LMER (−0.41) were higher than those of the HKA (−0.30). The adjusted R^2 for this analysis was 0.80 (Fig. 3). At each subgroup, the significant independent variables were the HKA and MMER at varus OA; HKA, MMER and LMER at valgus OA; and MMER at non-OA (Table 3). The prediction equation using significant independent variables at all subjects was as follows: medial ratio = 58.6 −

196 1.1 × HKA + 30.3 × MMER − 37.0 × LMER. In the regression analysis using only the HKA, the prediction

197 equation was as follows: medial ratio = 57.5 − 2.9 × HKA.

198 **Table 2.** Simple regression analysis to explore the correlation among the medial ratio, lower limb alignment,
199 and meniscus extrusion.

Variables	Medial ratio							
	All subjects		Varus OA		Valgus OA		Non-OA	
	R^2	P value	R^2	P value	R^2	P value	R^2	P value
HKA	0.63	<0.01	0.24	<0.01	0.11	0.26	0.01	0.77
mLDFA	0.36	<0.01	0.03	0.20	0.02	0.62	0.12	0.12
mMPTA	0.38	<0.01	0.12	0.01	0.01	0.77	0.01	0.70
MMER	0.45	<0.01	0.30	<0.01	0.03	0.56	0.21	0.05
LMER	0.47	<0.01	0.01	0.50	0.37	0.03	0.01	0.80

200

201

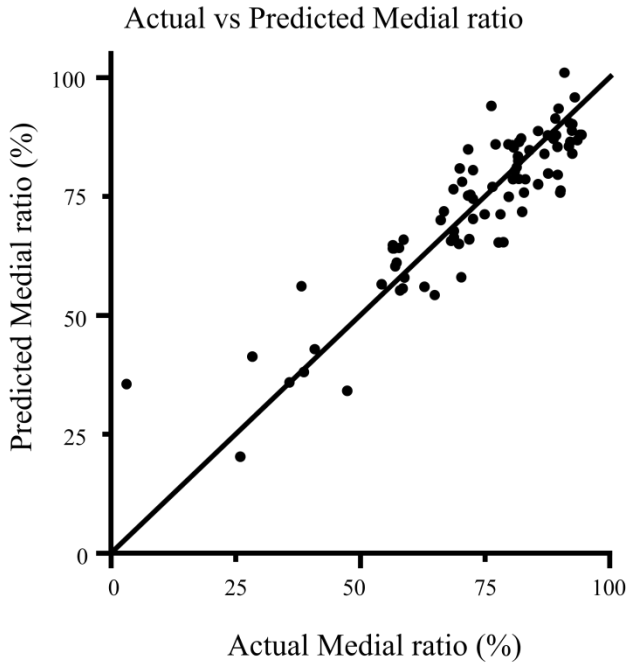

202 **Fig. 3.** Plot of the relationship between the actual and predicted values of the medial ratio across the data points
203 analyzed. The coefficient of determination (adjusted $R^2 = 0.80$) is provided as a measure of model fit, indicating
204 that the model explained 80% of the variance in the medial ratio.

205

Table 3. Multiple regression analysis of the influence on the medial ratio.

Variables	Medial ratio							
	All subjects (R^2 = 0.80, P< 0.01)		Varus OA (R^2 = 0.44, P< 0.01)		Valgus OA (R^2 = 0.55, P = 0.03)		Non-OA (R^2 = 0.26, P< 0.01)	
	β [95% CI]	p value	β [95% CI]	p value	β [95% CI]	p value	β [95% CI]	p value
HKA	−0.01 [−0.02, −0.01]	<0.01	−0.01 [−0.01, −0.003]	<0.01	−0.06 [−0.11, −0.01]	0.03	−0.01 [−0.02, 0.02]	0.97
mLDFA	0.01 [−0.02, 0.01]	0.76	0.01 [−0.01, 0.02]	0.45	0.04 [−0.11, 0.03]	0.24	−0.03 [−0.05, 0.01]	0.06
MMER	0.30 [0.21, 0.40]	<0.01	0.22 [0.12, 0.33]	<0.01	1.22 [0.08, 2.35]	0.04	0.73 [0.43, 1.47]	0.03
LMER	−0.38 [−0.50, −0.26]	<0.01	−0.15 [−0.38, −0.09]	0.23	−0.39 [−0.70, −0.07]	0.02	−0.35 [−1.15, 0.20]	0.38

β, regression coefficient; HKA, hip–knee–ankle; mLDFA, mechanical lateral distal femoral angle; MMER, medial meniscus-extrusion ratio; LMER; lateral meniscus-extrusion ratio.

Discussions

The results of this study showed that lower leg alignment and MER accounted for approximately 80% of the distribution of subchondral bone density. This finding indicates that 80% of the estimated stress distribution as assessed by CT-osteoabsorptiometry across the knee joint can be accounted for by lower leg alignment and meniscus extrusion. Lower leg alignment [6, 19] and meniscus injury [20-22] have been reported to be strong factors associated with stress distribution across the knee joint. The combination of these two strong factors has been thought to allow for an explanation of most of the distribution of subchondral bone density. The prediction equation for the medial ratio was 58.6 − 1.1 × HKA + 30.3 × MMER − 37.0 × LMER. For example, in a patient with typical varus OA and small HKA, high MMER, and low LMER, the medial ratio became high. In cases of medial meniscus posterior root tears, even when alignment is not strongly varus, the medial ratio also becomes high because of the high MMER. In non-OA knees, MMER and LMER are nearly normal. Thus, effects of MMER and LMER on the medial ratio in the prediction equation cancel each other out, resulting in the medial ratio being solely dependent on the HKA.

In this study, when the meniscus was not considered, the prediction equation for the medial ratio was 57.5 − 2.9 × HKA. A previous study using load sensor-integrated implants in TKA showed that the prediction equation was as follows: mediolateral force ratio = 63 − 2.6 × HKA [6]. This study showed that the prediction model (regression coefficient and intercept) of the medial ratio closely approximated that of the mediolateral force ratio from load sensor-integrated implants in TKA [6]. Data from load sensor-integrated implants can be used as a benchmark for the stress distribution across the knee joint, though these data do not reflect the meniscus function. A comparison between the prediction model of the CT-osteoabsorptiometry and that of load sensor-integrated implants showed that the distribution of subchondral bone density closely reflects the stress distribution. Nonetheless, the CT-osteoabsorptiometry has a primary limitation in that it does not directly measure the stress distribution.

KAM, which is calculated using 3D motion analysis, is a representative indicator of the medial-lateral load ratio in the knee joint [6, 19]. However, 3D motion analysis requires analytical equipment and specialized personnel. Thus, the facilities capable of this analysis are limited. Additionally, this method does not reflect the meniscus function, making it difficult to accurately estimate the actual stress distribution. Currently, evaluating the influence of the meniscus may be possible by combining 3D motion analysis with patient-specific finite element analysis [23, 24]. However, using this approach in a clinical setting is challenging. Conversely, the medial ratio can be calculated based on the results of this study using lower limb alignment and meniscus extrusion. Therefore, the stress distribution can be adequately assessed before and after surgery in routine clinical practice, even without the use of special devices. This method is valuable for future knee joint research.

The standardized regression coefficient of medial meniscus extrusion (MME) was higher than that of the HKA. This finding indicates that MME has a stronger impact on stress distribution than leg alignment. Lower leg alignment and meniscus tear independently influence the stress distribution [6, 19, 20, 25]. Furthermore, leg alignment can induce meniscus extrusion [26]. Therefore, the relationship between leg alignment, MME, and stress distribution is complicated. A biomechanical study showed that changes in lower leg alignment did not cause a statistically significant change in the mean contact pressure when the meniscus was in a normal state [27]. This finding indicates that the meniscus hoop function compensates for the effects of leg alignment on the stress distribution, indicating that the meniscus plays a significant role in the stress distribution. Based on these findings, the meniscus hoop function may be more important than alignment in influencing stress distribution. Therefore, reconstruction of the meniscus hoop function is an important part of the treatment strategy for knee OA.

In this study, subchondral bone was evaluated in both patients with OA and those without OA, regardless of varus or valgus alignment in the lower limbs. A previous study showed that pelvic width influenced KAM and that, even with the same alignment, pelvic width could affect the stress distribution [28]. Therefore, in this study, it might not be appropriate to categorize the stress distribution based solely on the alignment of the HKA of 0°. Furthermore, previous studies investigating the impact of alignment on KAM [19] and studies on TKA [6] have evaluated both varus and valgus alignments simultaneously. Therefore, we considered it appropriate to include both varus and valgus alignments without distinguishing between them.

Considering the mediolateral load distribution using KAM, an indicator of mediolateral load

distribution, the moment is the product of the ground reaction force (GRF) and the moment arm. The GRF vector rises from the center of pressure toward the center of mass, which is located anterior to the second sacral vertebra in a single-leg standing position [29]. Therefore, even with normal alignment, the medial compartment load is greater than lateral one. The medial compartment load increases further with varus alignment. Approximately 80% of the total load is distributed on the medial side at the HKA of 5° [6]. Conversely, even with valgus alignment, the medial load does not decrease drastically; at the HKA of 3°–5° valgus, the mediolateral load distribution is 50%:50% [6, 30]. Multiple regression analysis showed that the significant variables were the HKA and MMER at varus OA and HKA, MMER, and LMER at valgus OA. These results indicated that the mediolateral load distribution at valgus OA was influenced by not only LMER but also MMER because, even with valgus alignment, the load was distributed on the medial compartment, comparable to that on the lateral side.

This study has several limitations. First, although the CT-osteoabsorptiometry method is a valuable tool for estimating stress distribution across the knee joint, it does not directly measure stress distribution. Therefore, the findings of this study rely on the assumption that subchondral bone density reflects long-term loading patterns according to Wolff's law. Second, there is an inherent interaction between lower limb alignment and meniscus extrusion. As previously described, malalignment can influence meniscal position, and vice versa. This interrelationship may have affected the results of the multiple regression analysis. However, in this study, the variance inflation factors (VIF) for HKA and medial meniscus-extrusion ratio (MMER) were 2.1 and 1.7, respectively, indicating that multicollinearity was not substantial. Therefore, we believe that HKA and MMER

did not act as strong confounding variables in our analysis. Third, the OA and non-OA groups had different patient backgrounds. Non-OA patients were younger and likely had higher bone mineral density compared to older OA patients. However, since the medial ratio is defined as the proportion of the high-density area in the medial compartment relative to the total high-density area of both compartments, it is a relative measure that should not be substantially influenced by differences in absolute bone mineral density. Despite these limitations, this study provided important insights into the relationship between lower limb alignment, meniscus extrusion, and mediolateral load distribution via the distribution of subchondral bone density. These findings could contribute to a deeper understanding of load distribution across the knee joint and highlight key biomechanical factors that may be relevant for the prevention and treatment of osteoarthritis.

Conclusion

This study demonstrated that meniscus extrusion and lower leg alignment together explained approximately 80% of the variation in the distribution of subchondral bone density across the knee joint. The predictive model based on alignment parameters showed a similar trend to the mediolateral force ratio measured using sensor-integrated implants during TKA. These findings suggest that the distribution of subchondral bone density, as assessed by CT-osteoabsorptiometry, may reflect long-term joint stress distribution, and that this estimated distribution can be influenced by meniscus extrusion and lower leg alignment.

Acknowledgements

The authors would to thank Enago (www. enago. jp) for the English language review.

Acknowledgments

We are grateful to the staff of the Department of Orthopaedic Surgery, Faculty of Medicine and Graduated School of Medicine, Hokkaido University who gave of their time and expertise. Additionally, we would like to thank Enago (www. enago. jp) for editing a draft of this manuscript.

Author contributions

KI and TE conceived the project and designed the experiments. KI, TE, TS, YH, and MH collected and assembled data. EK and KI recruited patients. KI and TE prepared the draft of the manuscript. KI and TE secured funding for the project. DS, MM, TO, EK, and NI supervised the project. All authors critically reviewed the manuscript and provided their comments.

Role of the funding source

This work was supported by research grants from the Japan Society for the Promotion of Science (Grant-

in-Aid for Scientific Research; 24K12344 and 23K15729).

Conflict of interest/Competing interests

The institution of an author (KI) has received funding from Olympus Terumo Biomaterials CORP.

References

[1] Sharma L, Song J, Felson DT, Cahue S, Shamiyeh E, Dunlop DD. Functional Decline in Knee Osteoarthritis The Role of Knee Alignment in Disease Progression and The Role of Knee Alignment in Disease Progression and Functional Decline in Knee Osteoarthritis. JAMA 2001;2862862188:188-95. https://doi.org/10.1001/jama.286.2.188.

[2] Ghouri A, Muzumdar S, Barr AJ, Robinson E, Murdoch C, Kingsbury SR, et al. The relationship between meniscal pathologies, cartilage loss, joint replacement and pain in knee osteoarthritis: a systematic review. Osteoarthritis Cartilage 2022;30(10):1287-327. https://doi.org/10.1016/j.joca.2022.08.002.

[3] Pauwels F. Biomechanics of the Locomotor Apparatus. Berlin, Heidelberg: Springer Berlin Heidelberg; 1980.

[4] Hurwitz DE, Sumner DR, Andriacchi TP, Sugar DA. Dynamic knee loads during gait

predict proximal tibial bone distribution. J Biomech 1998;31(5):423-30. https://doi.org/10.1016/s0021-9290(98)00028-1.

[5] Wada M, Maezawa Y, Baba H, Shimada S, Sasaki S, Nose Y. Relationships among bone mineral densities, static alignment and dynamic load in patients with medial compartment knee osteoarthritis. Rheumatology (Oxford) 2001;40(5):499-505. https://doi.org/10.1093/rheumatology/40.5.499.

[6] Kutzner I, Bender A, Dymke J, Duda G, Von Roth P, Bergmann G. Mediolateral force distribution at the knee joint shifts across activities and is driven by tibiofemoral alignment. Bone and Joint Journal 2017;99B(6):779-87. https://doi.org/10.1302/0301-620X.99B6.BJJ-2016-0713.R1.

[7] Müller‐Gerbl M, Putz R, Kenn R. Demonstration of subchondral bone density patterns by three‐dimensional ct osteoabsorptiometry as a noninvasive method for in vivo assessment of individual long‐term stresses in joints. J Bone Miner Res 1992;7:S411-S8. https://doi.org/10.1002/jbmr.5650071409.

[8] Iwasaki K, Kondo E, Matsubara S, Matsuoka M, Endo K, Yokota I, et al. Effect of High Tibial Osteotomy on the Distribution of Subchondral Bone Density Across the Proximal Tibial Articular Surface of the Knee With Medial Compartment Osteoarthritis. Am J Sports Med 2021;49(6):1561-9.

https://doi.org/10.1177/03635465211002537.

[9] Fujie Y, Iwasaki K, Hamasaki M, Suzuki Y, Matsuoka M, Onodera T, et al. Paradoxical Change in Subchondral Bone Density in the Medial Compartment of the Proximal Tibial Articular Surface After High Tibial Osteotomy: A Detailed Subchondral Bone Density Analysis. Am J Sports Med 2024;52(9):2278-86. https://doi.org/10.1177/03635465241256100.

[10] Goto N, Okazaki K, Akiyama T, Akasaki Y, Mizu-Uchi H, Hamai S, et al. Alignment factors affecting the medial meniscus extrusion increases the risk of osteoarthritis development. Knee Surg Sports Traumatol Arthrosc 2019;27(8):2617-23. https://doi.org/10.1007/s00167-018-5286-7.

[11] Langhans MT, Lamba A, Saris DBF, Smith P, Krych AJ. Meniscal Extrusion: Diagnosis, Etiology, and Treatment Options. Curr Rev Musculoskelet Med 2023;16(7):316-27. https://doi.org/10.1007/s12178-023-09840-4.

[12] Gajjar SM, Solanki KP, Shanmugasundaram S, Kambhampati SBS. Meniscal Extrusion: A Narrative Review. Orthop J Sports Med 2021;9(11):23259671211043797. https://doi.org/10.1177/23259671211043797.

[13] Kellgren JH, Lawrence JS. Radiological assessment of osteo-arthrosis. Ann Rheum Dis 1957;16(4):494-502. https://doi.org/10.1136/ard.16.4.494.

[14] Yamaguchi J, Yasuda K, Kondo E, Kaibara T, Ueda D, Yabuuchi K, et al. Extrusion of the medial meniscus is a potential predisposing factor for post-arthroscopy osteonecrosis of the knee. BMC Musculoskelet Disord 2021;22(1):852. https://doi.org/10.1186/s12891-021-04730-7.

[15] Funakoshi T, Furushima K, Momma D, Endo K, Abe Y, Itoh Y, et al. Alteration of Stress Distribution Patterns in Symptomatic Valgus Instability of the Elbow in Baseball Players: A Computed Tomography Osteoabsorptiometry Study. Am J Sports Med 2016;44(4):989-94. https://doi.org/10.1177/0363546515624916.

[16] Onodera T, Majima T, Iwasaki N, Kamishima T, Kasahara Y, Minami A. Long-term stress distribution patterns of the ankle joint in varus knee alignment assessed by computed tomography osteoabsorptiometry. Int Orthop 2012;36(9):1871-6. https://doi.org/10.1007/s00264-012-1607-5.

[17] Shimizu T, Iwasaki N, Nishida K, Minami A, Funakoshi T. Glenoid stress distribution in baseball players using computed tomography osteoabsorptiometry: a pilot study. Clin Orthop Relat Res 2012;470(6):1534-9. https://doi.org/10.1007/s11999-012-2256-0.

[18] Miura S, Iwasaki K, Kondo E, Endo K, Matsubara S, Matsuoka M, et al. Stress on the posteromedial region of the proximal tibia increased over time after anterior

cruciate ligament injury. Knee Surg Sports Traumatol Arthrosc 2022;30(5):1744-51. https://doi.org/10.1007/s00167-021-06731-4.

[19] Hurwitz DE, Ryals AB, Case JP, Block JA, Andriacchi TP. The knee adduction moment during gait in subjects with knee osteoarthritis is more closely correlated with static alignment than radiographic disease severity, toe out angle and pain. J Orthop Res 2002;20(1):101-7. https://doi.org/10.1016/s0736-0266(01)00081-x.

[20] Bedi A, Kelly NH, Baad M, Fox AJ, Brophy RH, Warren RF, et al. Dynamic contact mechanics of the medial meniscus as a function of radial tear, repair, and partial meniscectomy. J Bone Joint Surg Am 2010;92(6):1398-408. https://doi.org/10.2106/JBJS.I.00539.

[21] Bedi A, Kelly N, Baad M, Fox AJ, Ma Y, Warren RF, et al. Dynamic contact mechanics of radial tears of the lateral meniscus: implications for treatment. Arthroscopy 2012;28(3):372-81. https://doi.org/10.1016/j.arthro.2011.08.287.

[22] Allaire R, Muriuki M, Gilbertson L, Harner CD. Biomechanical Consequences of a Tear of the Posterior Root of the Medial Meniscus. The Journal of Bone and Joint Surgery-American Volume 2008;90(9):1922-31. https://doi.org/10.2106/jbjs.G.00748.

[23] Park S, Lee S, Yoon J, Chae SW. Finite element analysis of knee and ankle joint

during gait based on motion analysis. Med Eng Phys 2019;63:33-41. https://doi.org/10.1016/j.medengphy.2018.11.003.

[24] Paz A, Orozco GA, Korhonen RK, García JJ, Mononen ME. Expediting Finite Element Analyses for Subject-Specific Studies of Knee Osteoarthritis: A Literature Review. Applied Sciences-Basel 2021;11(23). https://doi.org/ARTN 11440 10.3390/app112311440.

[25] Hunt MA, Birmingham TB, Bryant D, Jones I, Giffin JR, Jenkyn TR, et al. Lateral trunk lean explains variation in dynamic knee joint load in patients with medial compartment knee osteoarthritis. Osteoarthr Cartil 2008;16(5):591-9. https://doi.org/10.1016/j.joca.2007.10.017.

[26] Willinger L, Lang JJ, von Deimling C, Diermeier T, Petersen W, Imhoff AB, et al. Varus alignment increases medial meniscus extrusion and peak contact pressure: a biomechanical study. Knee Surg Sports Traumatol Arthrosc 2020;28(4):1092-8. https://doi.org/10.1007/s00167-019-05701-1.

[27] Willinger L, Lang JJ, Berthold D, Muench LN, Achtnich A, Forkel P, et al. Varus alignment aggravates tibiofemoral contact pressure rise after sequential medial meniscus resection. Knee Surg Sports Traumatol Arthrosc 2020;28(4):1055-63. https://doi.org/10.1007/s00167-019-05654-5.

[28] Iwasaki K, Ohkoshi Y, Hosokawa Y, Chida S, Ukishiro K, Kawakami K, et al. Higher Association of Pelvis-Knee-Ankle Angle Compared With Hip-Knee-Ankle Angle With Knee Adduction Moment and Patient-Reported Outcomes After High Tibial Osteotomy. Am J Sports Med 2023;51(4):977-84. https://doi.org/10.1177/03635465221150513.

[29] Peizer E. Human Locomotion. Bull Prosthet Res 1969;Fall:48-105. https://ci.nii.ac.jp/naid/10009780063/.

[30] Biehl M, Damm P, Trepczynski A, Preiss S, Salzmann GM. Towards planning of osteotomy around the knee with quantitative inclusion of the adduction moment: a biomechanical approach. J Exp Orthop 2021;8(1):39. https://doi.org/10.1186/s40634-021-00324-3.